

Graphite modified epoxy-based adhesive for joining of aluminium and PP/graphite composites

P. Rzeczkowski^a, P. Pötschke^a, M. Fischer^b, I. Kühnert^b, B. Krause^{a*}

^a Department of Functional Nanocomposites and Blends, Leibniz-Institut für Polymerforschung Dresden e.V., Hohe Str. 6, 01069 Dresden, Germany ^b Department of Processing, Leibniz-Institut für Polymerforschung Dresden e.V., Hohe Str. 6, 01069 Dresden, Germany

*corresponding author: krause-beate@ipfdd.de

For Peer Review Only

Graphite modified epoxy-based adhesive for joining of aluminium and PP/graphite composites

Abstract

A graphite-modified adhesive was developed in order to simultaneously enhance the thermal conductivity and the strength of an adhesive joint. The thermal conductivity through the joint was investigated by using highly filled PP/graphite composite substrates, which were joined with an epoxy adhesive of different layer thicknesses. Similar measurements were carried out with a constant adhesive layer thickness, whilst applying an epoxy adhesive, modified with expanded graphite (EG) (6, 10 and 20 wt%). By reducing the adhesive layer thickness or modifying the adhesive with conductive fillers, a significant increase in the thermal conductivity of the joint was achieved. The examination of the mechanical properties of the modified adhesives was carried out by tensile tests (adhesive only), lap-shear tests, and fracture energy tests (mode I) with aluminium substrates. Modification of the adhesive with EG led to an increase of the tensile lap-shear strength and the adhesive fracture energy (mode I) of the joint. In addition, burst pressure tests were performed to determine the strength of the joint in a complex component. The strength of the joint increased with the graphite content in the PP substrate and in the epoxy adhesive.

Keywords: mechanical properties of adhesives, conductive adhesives, epoxy/epoxides, aluminium and alloys, composites

1. Introduction

Thermally conductive adhesives find their application where good heat transfer at the junction of two components is required. Due to the high industrial demand, thermally conductive adhesives have been widely investigated to this day regarding their application in electronic devices [1-5]. A further application of thermally conductive adhesives is seals in heat exchangers where leak tightness against fluidic or gaseous media is needed. Limitations may be the mechanical properties with respect to the internal pressure that usually reaches several

1
2
3 bar. Since the development of fuel cells has increased significantly in recent years, driven by
4 environmental concerns and state subsidies to reduce air pollution and emission of CO₂, the
5 application of thermally conductive adhesives in fuel cells is of particular interest [6]. Fuel
6 cells have similar requirements as heat exchangers, except they usually do not operate at a
7 higher internal pressure than two bar. Therefore, the mechanical properties of the joint are not
8 a crucial concern. A proper seal with sufficient thermal conductivity and mechanical
9 properties is required to achieve easier and faster assembly and optimized operation.
10
11 Until now, only a few studies have been carried out in this field. In previous investigations
12 [7], a comprehensive research on the adhesive joining of highly filled PP/graphite composites
13 was outlined that indicated that this joining method is suitable for sealing purposes in fuel
14 cells. The potential industrial use of adhesive joining in fuel cells was reported in several
15 patents [8-12]. Since the materials and embodiments of heat exchangers and fuel cells are
16 very diverse [6, 13], adhesive joining has to be investigated for each particular application.
17 Because most of the adhesives are based on polymeric matrices with low intrinsic thermal
18 conductivity, there is a need to enhance matrix conductivity by using the addition of highly
19 conductive additives. Adhesives filled with diamond [1, 14], silver [1, 14-16], aluminium [1,
20 14, 16], ceramic [1, 14, 17] and carbon- based fillers [1, 18-20] are reported in literature.
21 Expanded graphite (EG) may be considered as a particularly interesting filler to increase the
22 thermal and electrical conductivities of polymers due to their low density, high surface area
23 and very good thermal and electrical properties. EG is created by the expansion of each
24 graphene layer in graphite crystallites where pores of different sizes exist between the layers.
25 This network of pores favors physical and chemical absorption of the polymer into the EG
26 particle that leads to better interconnection between adjusting particles. [21-23]
27
28 Thermally conductive adhesive is used to enhance the heat transfer through the joined area.
29
30 The heat transferred by a solid material is quantified by the heat flow \dot{Q} :
31
32
33
34
35
36
37
38
39
40
41
42
43
44
45
46
47
48
49
50
51
52
53
54
55
56
57
58
59
60

$$\dot{Q} = \frac{dQ}{dt} = -\lambda \cdot A \cdot \frac{dT}{dx} \quad (1)$$

where Q is the thermal energy, t the time, λ the thermal conductivity, A the cross-section area of the material and x the thickness of the material. The thermal conduction in polymer materials is caused primarily by phonons. Phonons are recognized as atom lattice vibrations, which allow the thermal energy to propagate within the polymer. The main reasons for low thermal conductivity of all polymers (usually 0.1-0.6 W/m·K) are their relatively low atom density, weak chemical interactions and bonds, complex crystal structure and irregularities in phonon transport. [24-27]

The heat transport through the adhesive joint depends not only on the thermal conductivity of the adhesive and substrate but on the interface as well. The phonon transport at the interface of two different phases is affected by the interruption of the crystal structure. Different densities and sound velocities at the interface result in an acoustic impedance mismatch which strongly impedes the phonon transport. This is explained by the acoustic mismatch model that determines the transmission coefficient of the phonon energy t_{AB} :

$$t_{AB} = \frac{4Z_A \cdot Z_B}{(Z_A + Z_B)^2} \quad (2)$$

where $Z = \rho c$ is the acoustic impedance, c the speed of sound, ρ the mass density and indices A and B the adjusting partners at the interface. When the phonons reach an interface, for instance, between the adhesive and the substrate or between the matrix and filler in a composite, they will be scattered. This effect is intensified by other surface defects (e.g. air voids). Poor phonon transfer and their scattering results in low thermal conductivity at the interface [26, 28]. Some authors investigated the thermal conductivity of epoxy-based adhesives where carbon based fillers were added. Burger et al. [25] measured an increase of the thermal conductivity of epoxy-based composites filled with 15 wt% EG compared to neat epoxy. Different values, depending on EG particles size, were achieved. An increase in thermal conductivity with increasing graphite content in an epoxy adhesive was reported

1
2
3 where the highest reported thermal conductivity was 1.68 W/m·K at 44.3 wt% graphite [1]. In
4
5 a recently published paper [29], an epoxy adhesive with 35 wt% EG and a thermal
6
7 conductivity of 2.5 W/m·K was presented. Moriche et al. [30] investigated the thermal
8
9 conductivity of an epoxy adhesive with an increasing graphene nanoplatelets (GNP) content
10
11 and achieved a value of 0.65 W/m·K at 10 wt% GNP. A significant increase of heat transfer
12
13 through an adhesive joint after functionalization of the interfaces adhesive/substrate was
14
15 reported by Sihn et al. in [31].
16
17

18
19 One of the concerns related to the modification of adhesive with conductive fillers is the
20
21 mechanical properties of the joint This is specially the case where carbon-based fillers at
22
23 higher contents are used. The mechanical properties of a composite are governed by the
24
25 properties of the filler and its shape, the polymer matrix, the adhesion between them and the
26
27 dispersion of the filler within the matrix [21, 32]. The strength of an adhesive joint depends
28
29 on the adhesion between the adhesive and the substrate, the load type and the intrinsic
30
31 strengths of the adhesive and the substrate material. The adhesion is of particular importance,
32
33 because it creates a bonding interface between the adhesive and the substrate. Adhesion
34
35 effects are formed by mechanical interlocking of the liquid adhesive in the micropores on the
36
37 adherend surface as well as chemical and physical bonds between the adhesive and the
38
39 substrate [33-34]. Gantayat et al. [35] have reported a gradual increase of the tensile stress at
40
41 break for epoxy/EG composites up to 9 wt% filler content and ascribed it to very good
42
43 dispersion of the filler. The addition of graphite to an epoxy resin has led to decreased tensile
44
45 lap-shear strength of a single overlap joint, as shown by [29, 36]. Li et al. [36] attributed it to
46
47 the shape of the graphite (particulate) and Kumar et al. [29] to the porous and layered
48
49 structure of EG. Results in [30] have shown, that the tensile lap-shear strength tended to
50
51 decrease after the addition of GNP. Different values were achieved -depending on the filler
52
53 content-, however, all values were below the initial strength of the neat adhesive. In [37],
54
55 epoxy adhesives filled with three different fillers were investigated: carbon nanotubes (CNT),
56
57
58
59
60

1
2
3 carbon nanohorns (CNH) and GNP. These modifications of an adhesive led to an increase of
4 tensile lap-shear strength of a single overlap joint up to 0.5-1.0 wt% filler content. Contrarily,
5 a decrease was reported in the case of higher filler content. This was caused by the creation of
6 filler agglomerates that resulted in a weaker interface with the epoxy matrix. The same effect
7 was reported in [38] for carbon black (CB)/epoxy adhesives where the tensile lap-shear
8 strength of a double lap joint increased up to 1.5 wt% CB and then decreased at higher values.
9
10 Incorporation of carbon nanofillers in an epoxy adhesive in [39] led to a slightly higher
11 adhesive fracture toughness, G_{IC} , on carbon fiber/epoxy composite substrates from 87.0 J/m²
12 for neat adhesive to 96.0 J/m² at 0.5 wt% carbon nanofibers (CNF) and 105.3 J/m² at 0.25
13 wt% CNT in the adhesive. In another work [40], the mixture of an epoxy adhesive with CNT
14 resulted in similar effects that lead to an increase in G_{IC} on an aluminium substrate. CNT
15 contents in the adhesive of 0.1, 0.3, and 0.5 wt% resulted in a respective increase of 22.8,
16 58.4, and 4.3 % compared to the neat adhesive. In [41], no distinct changes in mode I
17 adhesive fracture toughness of glass fiber epoxy composite substrates were reported after
18 addition of GNPs (0.25, 0.5 and 1.0 wt%) to the epoxy adhesive. Higher tensile-lap-shear
19 strength after the addition of carbon-based fillers may be due to two reasons i.e. increased
20 intrinsic strength of the adhesive or enhanced adhesion between the adhesive and the
21 substrate. In literature, a general trend could be found where initially the tensile strength of an
22 epoxy composite increases up to a certain amount of filler and then decreases at a higher filler
23 content due to the formation of agglomerates and/or poor adhesion between the filler and the
24 polymer matrix [42-45]. This corresponds well to the above-mentioned results from [37-38].
25
26 Better wetting of the substrate surface by the adhesive may cause the enhanced adhesion
27 between the adhesive and the substrate. In [30, 46], the contact angles on carbon fibre/epoxy
28 or aluminium substrates with carbon nanofibre (CNF) or GNP modified adhesives,
29 respectively, were decreased compared to neat epoxy.
30
31
32
33
34
35
36
37
38
39
40
41
42
43
44
45
46
47
48
49
50
51
52
53
54
55
56
57
58
59
60

1
2
3 This work focuses on the investigation and improvement of thermal conductivity and
4 mechanical properties of epoxy-based adhesives. For this purpose, an epoxy resin was
5 modified with expanded graphite (6, 10 and 20 wt% EG). The thermal conductivities of the
6 adhesive itself and through the adhesive joint (with highly filled PP/EG composite substrates)
7 for neat adhesive and EG modified adhesives were measured. Several mechanical tests were
8 carried out to investigate the influence of the EG content in the adhesive on the mechanical
9 properties of the adhesive and the adhesive joint. For this, tensile tests (adhesive only) and
10 tensile lap-shear tests as well as adhesive fracture toughness (mode I) tests on adhesively
11 bonded aluminium substrates were performed. In addition, burst air pressure tests up to 8 bar
12 were carried out on samples with a specially developed geometry. Thermogravimetric
13 analysis and optical microscopy were conducted in order to examine the actual graphite
14 content and graphite particle distribution in the adhesives.

2. Materials and methods

2.1. Materials

36 Commercially available low-viscosity epoxy resin Epikote MGS RIMR 145 mixed with the
37 curing agent (hardener) Epikote MGS RIMH 145 and the catalyst Epikote MGS RIMC 145
38 (all from Hexion Inc., Columbus, OH, US) at a respective ratio of 100, 82 and 0.5 parts by
39 weight was used as an adhesive. Expanded graphite Sigratherm GFG5 (EG GFG5) (from SGL
40 Carbon, Meitingen, Germany) with a particle size of $x_{10} = 2.3 \mu\text{m}$, $x_{50} = 6.4 \mu\text{m}$ and $x_{90} = 15.0$
41 μm was utilized as thermally conductive filler for the modification of the adhesive. Neat and
42 graphite modified adhesives were cured at 90 °C for 16 h in a heating oven.

43 The substrate materials for mechanical testing of the adhesive joints (lap-shear and fracture
44 toughness tests) were made of aluminium alloy AW-2024. For the measurements of the
45 thermal conductivity through the joint as well as for the burst pressure tests,
46 polypropylene/graphite composite substrates were used, in which polypropylene (PP) Sabic
47
48
49
50
51
52
53
54
55
56
57
58
59
60

1
2
3 579S (Sabic, Riyadh, Saudi Arabia) with a melt flow rate of 47 g/10min at 260 °C/2.16 kg
4
5 was used as the polymer matrix. As substrate material for the burst pressure test, neat PP or
6
7 PP/graphite composites that contain the synthetic graphite Timcal Timrex KS500 (from
8
9 Imerys Graphite & Carbon, Bironico, Switzerland) were used. For the measurement of the
10
11 thermal conductivity through the joint, PP composite filled substrates with expanded graphite
12
13 Sigratherm GFG600 (EG GFG600) (from SGL Carbon, Meitingen, Germany) with a particle
14
15 size of $x_{10} = 106 \mu\text{m}$, $x_{50} = 269 \mu\text{m}$, $x_{90} = 395 \mu\text{m}$ and $x_{99} = 444 \mu\text{m}$ [47] were used.
16
17
18
19

20 **2.2. Processing methods**

21
22
23 The PP-based composite substrate, containing 60 wt% of EG Sigratherm GFG600, was used
24
25 for the measurements of the thermal conductivity through the joint. For the melt mixing, a
26
27 twin-screw extruder Berstorff ZE 25 (KraussMaffei Berstorff GmbH, Hannover, Germany)
28
29 with a screw diameter D of 25 mm, a screw length of 48D and a temperature profile from 180
30
31 to 200 °C as described in [7] was used. Thin plates with the size of 80 mm x 80 mm x 0.8 mm
32
33 were compression molded using a hot press Paul-Otto Weber PW40EH (Paul-Otto Weber,
34
35 Remshalden, Germany) (240 °C, 50 kN, 2.5 min).
36
37
38
39

40
41 The epoxy adhesive was mixed with 6, 10 and 20 wt% EG Sigratherm GFG5 using a
42
43 magnetic stirrer. The 6 and 10 wt% of EG GFG5 were added directly to the three component
44
45 mixture (resin, hardener, catalyst), mixed with a magnetic stirrer (250 rpm, 3 h) followed by
46
47 degassing in a vacuum chamber for 15 min. The content of 20 wt% had to be pre-mixed with
48
49 acetone after mixing EG GFG5 directly with the epoxy resin due to the very high viscosity.
50
51 Firstly, only one component (resin) was added to the EG GFG5/acetone mixture and stirred
52
53 by using a magnetic stirrer for 3 h at 250 rpm followed by slow stirring at 50 °C at 50 rpm for
54
55 24 h and degassing in a vacuum oven for 3 h at 50 °C in order to remove acetone residues.
56
57 Then the hardener/catalyst mixture was added and mixed for a few minutes to form a pasty
58
59
60

1
2
3 adhesive. TGA measurements were carried out in order to determine the actual EG content in
4 the modified epoxy adhesives. The results are summarized in Table 1. It was determined that
5 the actual filler content in the adhesives are very close to the set-up values.
6
7
8

9
10
11 PP/graphite composites that contain 20, 40, or 60 wt% graphite Timcal Timrex KS500 were
12 prepared at 200°C by using a co-rotating twin screw extruder ZSK 26 Mc (Coperion GmbH,
13 Stuttgart, Germany) at RWTH Aachen. The screw diameter, D , and extrusion length were 26
14 mm and 44 D , respectively. A rotation speed of 150 rpm and a throughput of 10 kg/h were
15 maintained [48]. The samples for the burst pressure tests comprised of neat PP and
16
17
18
19
20
21
22
23
24
25
26
27
28
29
30
31
32
33
34
35
36
37
38
39
40
41
42
43
44
45
46
47
48
49
50
51
52
53
54
55
56
57
58
59
60
PP/graphite KS500 composites were injection molded at 235-275 °C by using an Allrounder
420C 1000-250 injection molding machine (Arburg GmbH+Co. KG, Loßburg, Germany)
with a mold temperature of 20-40 °C, whereas the temperatures were increasing with filler
content in the composite. The upper shell was manufactured with a key-shaped joining
surface and the lower shell with a groove-shaped joining surface. The samples were designed
in such a way, that a gap for the adhesive is created between the feather key and the groove so
that the two surfaces could be joined after they had been brought together (Figure 3). Similar
samples for determination of the strength against internal pressure of polymer composites
were previously reported in [49].

2.3. Adhesive joining

To measure the thermal conductivity through the joint, two compression molded PP/60 wt%
EG GFG600 plates (each 0.8 mm thick) were adhesively joined with neat epoxy adhesive or
adhesives modified with EG GFG5. The surfaces to be joined were roughened with abrasive
paper with a P600 fineness and cleaned with ethanol prior to joining in order to remove the
thin polymer layer after compression molding. Different adhesive layer thicknesses were
adjusted with neat adhesive: 0.1, 0.3 and 0.5 mm to determine influence of adhesive layer

1
2
3 thickness on the thermal conductivity through the joint (Figure 2). Joints with graphite-
4 modified adhesives were prepared with a constant adhesive layer thickness of 0.5 mm, but
5 with increasing EG GFG5 content in the adhesive: 6, 10 and 20 wt% to investigate the
6 influence of the filler content in the adhesive on the thermal conductivity through the joint.
7
8
9
10
11
12

13 The samples for the lap-shear tests were prepared in accordance with DIN EN 1465 by using
14 aluminium strips (AW-2024) with the dimensions 100 mm x 25 mm x 1.6 mm and joined to
15 form single lap joints with an overlap length of 12.5 mm and an adhesive layer thickness of
16 0.2 mm (Figure 1). The surfaces to be joined were sand-blasted and cleaned with acetone
17 prior to joining.
18
19
20
21
22
23
24
25

26 The samples for the determination of the adhesive fracture energy were joined in accordance
27 with ISO 25217:2009 to form double cantilever beams (DCB) in mode 1, using aluminium
28 alloy AW-2024 strips with the dimensions 200 mm x 25 mm x 4 mm. A PTFE insert film
29 with a length of 60 mm and thickness of 10 μm was inserted to create a defined pre-crack.
30 The measured adhesive layer thickness of the joined samples was 0.35 mm. To enable the
31 clamping, two aluminium blocks (25 mm x 20 mm x 10 mm, including holes with a diameter
32 of 4.5 mm) were bonded to the ends of the sample where the PTFE films were inserted
33 (Figure 1). The surfaces to be joined were sandblasted and cleaned with acetone prior to
34 joining.
35
36
37
38
39
40
41
42
43
44
45
46
47

48 The samples for the burst pressure tests, made of neat PP or PP-based composites containing
49 20, 40 or 60 wt% graphite Timcal Timrex KS500, were adhesively joined using the neat
50 epoxy adhesive and EG GFG5 modified epoxy adhesives. The surfaces to be joined were
51 sandblasted and cleaned with ethanol prior to joining. After application of the adhesive in the
52 groove, both parts were brought together and pressed with a foldback clip (compression force
53 about 7.9 N) on each edge (Figure 3).
54
55
56
57
58
59
60

2.4. Characterization methods

The thermogravimetric analysis (TGA) of the EG GFG5 modified adhesives was conducted using a TGA Q5000 (TA Instruments, New Castle, DE, US) between 25 and 800 °C under nitrogen atmosphere at a scan rate of 10 K/min. The same samples as for thermal conductivity measurements of the adhesives were used.

The size distribution of the graphite powders was determined by laser diffraction with a HELOS/BF particle size analyzer coupled to a RODOS dry dispersion unit (Sympatec GmbH, Clausthal-Zellerfeld, Germany) and an ASPIROS microdosing module (Sympatec GmbH, Clausthal-Zellerfeld, Germany). The measuring range was 4.5–875 µm (EG GFG600) or 0.5–170 µm (EG GFG5).

The through-plane thermal conductivity was measured at 25 °C using the laser flash method with a device LFA 447 (Netzsch GmbH, Selb, Germany). The given values are mean values of three measurements. The samples for the determination of the thermal conductivity of the neat adhesive and EG GFG5 modified adhesives were casted in a PTFE mold to a round shape with a diameter of 12.7 mm and a thickness of 2.0 mm. The samples for the measurements of the thermal conductivity through the joint were cut from the adhesively joined composite plates (see section 2.3) to square samples with an edge length of 12.7 mm (Figure 2).

The tensile tests of the adhesives and the lap-shear tests of adhesively joined aluminium strips were carried out using a Zwick Roell 1456 universal testing machine (Zwick Roell Group, Ulm, Germany) and the adhesive fracture toughness test (double cantilever beam (DCB) mode 1) using the Zwick Roell Z010 (Zwick Roell Group, Ulm, Germany) testing machine.

The lap-shear tests were carried out with a speed of 1 mm/min and the tensile tests and adhesive fracture toughness tests with a speed of 5 mm/min. The samples for tensile tests

1
2
3 were milled from cast plates (80 mm x 80 mm x 0.8 mm) in order to obtain samples of size
4
5 1BA according to DIN EN ISO 527-2. The adhesive fracture energy (G_{IC}) was calculated by
6
7 applying the corrected beam theory (CBT) according to ISO 25217 using the force (P), crack
8
9 length (a) and displacement of the cross-head of the machine (δ) obtained from the test:
10
11
12

$$G_{IC} = \frac{3P\delta}{2B(a + |\Delta|)} \cdot \frac{F}{N} \quad (3)$$

13
14
15
16 where B is the width of the specimen, Δ the crack length correction, F the large-displacement
17
18 correction and N the load-block correction. The fracture energy G_{IC} was calculated for several
19
20 crack lengths for each specimen and a mean value for each sample was calculated.
21
22
23

24
25 The burst pressure tests were conducted using a standard air pressure regulator. One of the
26
27 inlets was cut to connect the sample with a pneumatic fitting and an air hose to apply the air
28
29 pressure. The maximum applied air pressure was 8 bar. Firstly, samples were immersed in a
30
31 closed water vessel and pressurized at 2 bar for 1 minute to check the gas-tightness of the
32
33 adhesively joined samples (Figure 3). Then, air pressure was slowly increased up to 8 bar and
34
35 held for 1 minute to determine the burst air pressure.
36
37
38

39
40 Optical microscopy was carried out with an Olympus BX53M coupled with a camera
41
42 Olympus D71 (both Olympus GmbH, Hamburg, Germany). Thin sections were cut with a
43
44 diamond knife at room temperature from the same samples used for the measurement of the
45
46 thermal conductivity of the adhesives.
47
48
49

50 **3. Results and discussion**

51 **3.1. Thermal conductivity (through-plane)**

52 **3.1.1. Thermal conductivity of the adhesives**

53
54
55
56
57
58
59
60

1
2
3 The thermal conductivity of the neat epoxy adhesive and the modified adhesives containing 6,
4 10 or 20 wt% EG GFG5 was measured in order to examine the impact of the filler content on
5 the thermal conductivity. It can be seen from Figure 4 that the thermal conductivity increases
6 almost linearly with the EG GFG5 content in the adhesive. The highest thermal conductivity
7 of 0.93 ± 0.03 W/m·K was measured for the adhesive containing 20 wt% EG GFG5 indicating
8 an increase of nearly 300% compared to the neat adhesive (0.23 ± 0.01 W/m·K). The increase
9 of thermal conductivity after addition of EG particles to the adhesive is caused by the
10 increased phonons transport through the composite structure.
11
12
13
14
15
16
17
18
19
20
21
22

23 These results are comparable to those reported in [25] where an increase in thermal
24 conductivity of epoxy/EG composites to values of 0.45, 0.7, and 1.7 W/m·K were measured
25 after addition of 5, 10, and 23 wt% EG, respectively. In [1], a conductivity of about 0.75
26 W/m·K at 27 wt% graphite was reported. Higher values were only achieved after mixing
27 epoxy adhesives with much higher graphite contents such as 43 wt% graphite (1.68 W/m·K)
28 [1] and 35 wt% EG (2.5 W/m·K) [29].
29
30
31
32
33
34
35
36
37

38 3.1.2. Thermal conductivity through the joint

39
40 The thermal conductivity through the joint was measured to investigate the influence of
41 adhesive layer on the thermal conductivity through the two adhesively joined substrates. The
42 thermal conductivity of the substrate material (PP + 60 wt% EG GFG600) is 9.47 ± 0.33
43 W/m·K [7] and that of the neat adhesive is 0.23 ± 0.01 W/m·K.
44
45
46
47
48
49
50

51 Firstly, the thermal conductivity through the joint with varying adhesive layer thicknesses
52 (0.1, 0.3 and 0.5 mm) was measured by using a neat adhesive, as shown in Table 2. A strong
53 dependency of the thermal conductivity through the joint on the adhesive layer thickness is
54 observed. The adhesive layer seems to significantly impede the thermal conductivity through
55 the joint. By reducing the adhesive layer thickness from 0.5 mm to 0.1 mm, the thermal
56
57
58
59
60

1
2
3 conductivity through the joint is increased from 0.87 ± 0.07 W/m·K to 2.09 ± 0.30 W/m·K,
4
5 which corresponds to an increase of approx. 140%.
6
7

8
9 Secondly, the thermal conductivity through the joint with a constant adhesive layer thickness
10 (0.5 mm) by using a modified epoxy adhesive containing 6, 10 or 20 wt% EG GFG5 was
11 measured. By mixing the adhesive with the conductive filler resulted in a gradual increase of
12 the thermal conductivity through the joint with increasing filler content (Figure 5). The
13 addition of only 6 wt% EG GFG5 to the adhesive led to a significant increase in the thermal
14 conductivity through the joint i.e. from 0.87 ± 0.07 W/m·K (neat adhesive) to 1.9 ± 0.27
15 W/m·K (6 wt% EG GFG5 in adhesive), whilst the addition of 20 wt% EG further increases it
16 to 3.36 ± 0.05 W/m·K.
17
18
19
20
21
22
23
24
25
26
27

28 These results prove that the increase in thermal conductivity is not only possible by reducing
29 the thickness of the adhesive layer but also by adding a small amount of conductive fillers to
30 the adhesive. The increase of thermal conductivity through the joint may be caused by
31 increased heat transfer through the adhesive layer and by reducing the acoustic impedance
32 mismatch in the interface adhesive/substrate after addition of EG to the adhesive. This leads
33 to better thermal transport at the adhesive/substrate interface and therefore through the entire
34 joint [26, 31, 50-51]. This is confirmed by the analysis of the percental increase of the thermal
35 conductivities of the adhesive itself and through the joint after addition of EG GFG5. The
36 increase of thermal conductivity through the joint for adhesives with 6 and 10 wt% EG GFG5
37 is twice as high as for the adhesive itself. The reason for this effect may be the particles of
38 expanded graphite in both the adhesive and the substrate, which can reduce the acoustic
39 impedance mismatch through the interface of two adjacent phases. It is noticeable that the
40 increase of the thermal conductivity through the joint for the adhesive with 20 wt% EG GFG5
41 is less pronounced than that of the adhesives with lower EG content. This may be caused by
42 higher porosity of the adhesive with 20 wt% EG GFG5 and more air voids at the adhesive-
43
44
45
46
47
48
49
50
51
52
53
54
55
56
57
58
59
60

1
2
3 substrate interface and hence a less efficient heat transfer through the joint. The mixing of the
4 epoxy resin with 20 wt% EG GFG5 led to a substantial increase in viscosity of the mixture
5 that formed a pasty adhesive, which prevented degassing prior to the adhesive application (see
6 section 3.3).
7
8
9
10

11
12
13 Sihm et al. [31] reported on the thermal conductivity through the two with epoxy resin fused
14 graphite facesheets. The vertically aligned MWCNTs were placed on one side of the adhesive
15 film. Subsequently, both sides of the adhesive film and both the substrate surfaces to be
16 bonded, were pre-coated with a few conductive metallic thin layers. Two graphite facesheets
17 were then fused together with the modified adhesive film. This functionalization of the
18 interface between the adhesive and the substrate has been used to reduce the acoustic
19 impedance mismatch and phonon scattering at the interface to achieve more effective phonon
20 transport. This resulted in an extreme increase of the thermal conductivity through the joint
21 from 0.79 W/m·K (non-functionalized, neat epoxy adhesive film) to 250.4 W/m·K
22 (MWCNT/epoxy adhesive layer with functionalized interfaces).
23
24
25
26
27
28
29
30
31
32
33
34
35

36 37 **3.2. Mechanical properties**

38 39 **3.2.1. Tensile strength and tensile lap-shear strength of the adhesives**

40
41 The tensile test was carried out in order to examine the impact of the EG GFG5 addition on
42 the tensile strength of the adhesive itself. Figure 6 shows the effect of increasing EG GFG5
43 content in the epoxy adhesive on its tensile strength. The tensile strength decreases almost
44 linearly with increasing filler content from 77.3 MPa (neat adhesive) to 43.3 MPa (adhesive
45 with 20 wt% EG GFG5). The reduced tensile strength is caused by the incorporation of
46 brittle, low intrinsic strength EG particles within the epoxy matrix. This is caused by easy
47 shearing and gliding between graphene layers within a graphite crystallite. [21] Another
48 reason for decreased strength of the EG modified adhesives may be their lower degree of
49
50
51
52
53
54
55
56
57
58
59
60

1
2
3 curing [52-53]. As shown in [52, 54-55], the addition of carbon-based fillers to an epoxy
4 matrix can lead to a lower final degree of curing of the composite. Since the filler was not
5 functionalized, poor adhesion and non-optimal interface between EG particles and epoxy
6 matrix lead to impaired cohesion within the adhesive resulting in lower tensile strength [21,
7 56]. In [36], a similar effect was reported for the addition of graphite to an epoxy resin. The
8 tensile strength gradually decreased with increasing filler content up to 25 wt%. However,
9 different results were achieved with EG or GNP in [35, 57]. Gantayat et al. [35] reported a
10 gradual increase of tensile strength of EG/epoxy composites up to 9 wt% EG; achieving 40
11 MPa at this filler content. In [57], the tensile strength of the epoxy composites filled with
12 graphite platelets (GP) increased up to 41 MPa at 2.5 wt% GP and decreased at 5 wt% GP to
13 37.5 MPa, but still remained above the tensile strength of neat epoxy (34 MPa).
14
15
16
17
18
19
20
21
22
23
24
25
26
27
28
29

30 The next step of the evaluation the EG GFG5 modified epoxy adhesives was the investigation
31 of the tensile lap-shear strength on adhesively joined aluminium substrates. Figure 6 shows
32 the effect of increasing filler content in the adhesive on the tensile lap-shear strength. The
33 addition of EG GFG5 particles to the adhesive leads to an almost linear increase of the tensile
34 lap-shear strength and achieves its highest value of 11.1 ± 0.3 MPa at 20 wt% EG GFG5. This
35 represents an increase of nearly 48% compared to the tensile lap-shear strength of the neat
36 epoxy adhesive (7.5 ± 0.4 MPa). By comparing values of the tensile strength of the adhesive
37 with tensile lap-shear strength of the joint it can be seen, that decreasing tensile strength does
38 not impair the tensile lap-shear strength of the joint.
39
40
41
42
43
44
45
46
47
48
49
50

51 An important change can be observed from the fracture surface analysis of the samples. In
52 Figure 7, three kinds of failure patterns can be seen: adhesive failure, cohesive failure and
53 mixed failure (adhesion/cohesion failure). Adhesive failure indicates an insufficient adhesion
54 between the adhesive and the substrate. Contrarily, cohesive failure means that the interfacial
55 strength surpasses the intrinsic strength of the adhesive and leads to the loss of coherence
56
57
58
59
60

1
2
3 within the adhesive layer. Mixed failure is a mix of both above-mentioned failure modes
4
5 where cohesive and adhesive areas on the fracture surface can be recognized. With increasing
6
7 EG GFG5 content in the adhesive, the failure type of the joint changes from adhesive failure
8
9 to cohesive failure. However, the samples joined with neat adhesive or adhesive modified
10
11 with 6 wt% EG GFG5 fractured adhesively in the interface between the adhesive and
12
13 substrate. The 10 wt% EG GFG5 led to a mixed failure with a predominant part of adhesive
14
15 failure. This mixed failure mode may be the reason for the relatively high standard deviation
16
17 of the tensile lap-shear strength values. The percentage of cohesive failure in the total fracture
18
19 surface varied among the five tested samples. The adhesive modified with 20 wt% EG GFG5,
20
21 which provided the highest tensile lap-shear strength, failed fully cohesively within the
22
23 adhesive layer. This conversion of the failure mode indicates that the incorporation of EG
24
25 particles in the epoxy adhesive may lead to enhanced adhesion and stronger interface between
26
27 the adhesive and the aluminium surface. The strength of the interface surpassed the strength
28
29 of the adhesive itself that lead to the cohesive failure within the adhesive layer (with 20 wt%
30
31 EG GFG5) and thereby to an increase of the tensile lap-shear strength.
32
33
34
35
36
37
38

39 The EG GFG5 modified adhesives from this work provided better mechanical properties
40
41 compared to some previous work where the tensile lap-shear strength on aluminium substrates
42
43 decreased after addition of carbon nanofillers to an epoxy adhesive. In [29], lower tensile lap-
44
45 shear strengths of the modified adhesives of 2.5 MPa (epoxy + 35 wt% EG) and 2.8 MPa
46
47 (epoxy + 35 wt% EG/GNP) were measured compared to the neat adhesive (4.05 MPa).
48
49 Similar effects were also reported in [30] where an epoxy adhesive filled with different GNP
50
51 contents resulted in lower tensile lap-shear strength than the neat adhesive. It ranged from 7.3
52
53 to 8.0 MPa depending on filler content compared to 8.3 MPa for the neat adhesive.
54
55
56
57

58 3.2.2. Adhesive fracture toughness (mode I)

59
60

1
2
3 Figure 8 shows the fracture energy values (G_{IC}) for single specimens of aluminium substrates
4 as a function of the crack length (a) along the adhesive layer. It can be seen that the EG GFG5
5 modified adhesives exhibit much higher fracture energy than the neat epoxy adhesive. The
6 fracture energies of all adhesives filled with EG GFG5 remain more or less in the same range
7 independently of EG content in the adhesive. This corresponds to the increase in the tensile
8 lap-shear strength with increasing EG content in the adhesive (see section 3.2.1).
9

10
11 For the EG filled adhesives, some variations in fracture energy along the crack length could
12 be observed. These deviations can be correlated with the failure mode of the joint. The
13 analysis of the fracture surface along the crack length in the samples with mixed failure type
14 (adhesives with 6 and 10 wt% EG GFG5) led to the conclusion that the fracture energy tends
15 to increase at locations in the samples where cohesive fracture areas start or increase and
16 where the adhesive fracture areas get smaller. Further observation of the fracture surfaces
17 revealed a relatively high porosity with non-uniform distribution of air voids within the
18 adhesive layer that may be another reason for the fracture energy deviations.
19
20
21
22
23
24
25
26
27
28
29
30
31
32
33
34
35
36

37 Table 3 lists the results of the adhesive fracture energies for all specimens. These G_{IC} values
38 may be considered as low in comparison with some previous works [40, 58]. Already the
39 addition of 6 wt% EG GFG5 to the adhesive resulted in a significant increase of fracture
40 energy compared to the neat adhesive. However no further distinct changes in fracture energy
41 could be observed with increasing EG GFG5 content in the adhesive. All samples showed
42 relatively high deviations of the measured values that can be ascribed to the change of the
43 fracture type or the observed porosity within the adhesive layer. Figure 9 shows pictures of
44 the fracture surfaces of all adhesives. While unmodified epoxy adhesive fractured fully
45 adhesively, mixed failure is observed on the fracture surfaces of the adhesive with 6 wt% EG
46 GFG5. Distinct cohesive failure areas could be seen, although with a predominant adhesive
47 fracture part. Higher EG GFG5 content in the adhesive (10 wt%) led to larger cohesive failure
48
49
50
51
52
53
54
55
56
57
58
59
60

1
2
3 areas and just some small areas with adhesive failure could be found along the edge of the
4 specimen. The adhesive containing 20 wt% EG fractured fully cohesively within the adhesive
5 layer. The change of failure mode indicates that higher adhesive fracture toughness achieved
6 with EG GFG5 modified adhesives may have been caused by enhanced adhesion between the
7 adhesive and the aluminium substrate. These results are consistent with the results of the
8 tensile lap-shear strength tests described in section 3.2.1. Very similar changes of the failure
9 mode with increasing EG GFG5 content in the adhesive were observed.

10
11
12
13
14
15
16
17
18
19
20
21
22
23
24
25
26
27
28
29
30
31
32
33
34
35
36
37
38
39
40
41
42
43
44
45
46
47
48
49
50
51
52
53
54
55
56
57
58
59
60
The increase in adhesive fracture energy through reinforcing of epoxy adhesives with carbon
nanofillers has already been reported, but not yet with EG. As described in [40], the adhesive
fracture energy G_{IC} on aluminium substrates increased from 299.7 J/m² for neat adhesive to
474.9 J/m² with the addition of 0.3 wt% CNT in the adhesive. At higher filler content, G_{IC}
decreased to a value of 312.6 J/m² very close to G_{IC} of the neat adhesive. A similar effect was
reported on carbon fiber/epoxy substrate where an epoxy/0.25 wt% CNT adhesive resulted in
a higher G_{IC} value of 105.3 J/m² compared to the neat adhesive (87.0 J/m²) [39].

3.2.3. Burst pressure test

The results of the burst pressure test are summarized in Table 4. Samples made of neat PP
joined with neat epoxy adhesive failed at lower air pressure (3.5 or 5 bar) compared to
samples made of PP composites containing 20 wt% graphite KS500 that could provide better
performance and survived exposure to higher internal air pressure (failure at 4 bar or no
failure). Substrates containing 40 and 60 wt% graphite KS500 joined with neat adhesive did
not fail at all at 8 bar after 1 min. It can be concluded from these results that increasing
graphite content in PP-based composites leads to better adhesion between the epoxy adhesive
and the substrate that resulted in higher resistance against internal air pressure. This may have
been caused by higher porosity of the PP/graphite KS500 substrate surface compared to the

1
2
3 neat PP substrate. The neat adhesive with low viscosity could fill the micropores on the rough
4
5 surface of PP/graphite KS500 substrate that lead to better mechanical anchoring of the
6
7 adhesive. Another reason may have been, as reported in [7], increasing surface tension of the
8
9 substrate with increasing graphite content in the PP matrix that leads to better wetting of the
10
11 surface by the adhesive. Better wetting properties of the surface allow the molecules of the
12
13 adhesive and the substrate surface to come closer to each other, which is one of the
14
15 preconditions for good adhesion and therefore higher strength of the joint.
16
17
18
19

20 The efficiency of the EG GFG5 modified adhesives in burst pressure tests was also examined.
21
22 With increasing EG GFG5 content in the epoxy adhesive, the adhesively joined samples can
23
24 survive exposure to higher internal air pressure (Table 4). While samples joined with the
25
26 adhesive containing 6 wt% EG GFG5 withstood slightly higher air pressure than the neat
27
28 epoxy adhesive, the adhesive with 10 wt% EG GFG5 failed only at maximal air pressure of 8
29
30 bar after 30 sec. The adhesive with 20 wt% EG GFG5 failed at lower air pressure (7 bar) than
31
32 the adhesive with 10 wt% EG GFG5, but still withstood higher air pressure than the neat
33
34 adhesive. Similar effects of deterioration of mechanical properties at higher filler contents
35
36 were reported in [37-38] where the strength of the joint increased up to a certain filler content
37
38 (CNT, GNP or carbon black) in the adhesive and then decreased at a higher filler content. It
39
40 can be concluded that the incorporation of EG GFG5 in the epoxy adhesive provides stronger
41
42 adhesion not only to aluminium but also to PP substrates.
43
44
45
46
47
48
49
50
51

52 **3.3. Optical microscopy**

53
54
55 To evaluate the distribution of the EG GFG5 particles in the epoxy matrix, thin cross sections
56
57 of modified adhesives were studied by using optical transmission microscopy. Figure 10
58
59 shows micrographs illustrating the distribution of EG GFG5 in the epoxy matrix. Dark
60

1
2
3 regions represent EG particles and white regions the epoxy component. In the micrographs an
4
5 uniform dispersion of the EG GFG5 particles in the epoxy matrix can be seen. No distinct
6
7 agglomerates of EG GFG5 could be observed. In the micrograph of the adhesive with 20 wt%
8
9 EG, the large roundly shaped white spots are identified as air voids that could be found in
10
11 almost every area of the thin sections. This is an effect of the very high viscosity of the
12
13 adhesive after mixing with the EG powder that prevented degassing of the adhesive prior to
14
15 placing it in the casting mold.
16
17
18
19
20

21 **4. Conclusions**

22
23 In this study, the thermal conductivity through the joints on PP/EG GFG600 composites with
24
25 epoxy adhesives and the mechanical properties of adhesive joints on aluminium and
26
27 PP/graphite substrates, were investigated. Moreover, the effect of the incorporation of fillers
28
29 in the epoxy-based adhesive with expanded graphite (EG) was investigated.
30
31

32
33 With increasing EG GFG5 content in the adhesive (6, 10 and 20 wt%), higher through-plane
34
35 thermal conductivity of the adhesive was achieved. The maximum value reached 0.95 W/m·K
36
37 at 20 wt% EG GFG5. The thermal conductivity through the joint on the highly filled PP/EG
38
39 GFG600 substrate, with an adhesive layer thickness of 0.5 mm was increased from 0.87
40
41 W/m·K for the neat adhesive to 3.36 W/m·K for the adhesive containing 20 wt% EG GFG5.
42
43 Furthermore, a strong dependency of the thermal conductivity through the joint on the
44
45 adhesive layer thickness with neat epoxy adhesive could be observed.
46
47
48

49
50 An increase in EG GFG5 content in the epoxy resin led to a lower tensile strength of the
51
52 adhesive due to the low intrinsic strength of the EG or poor adhesion between the EG and the
53
54 polymer matrix. The adhesives filled with EG GFG5 showed a higher tensile-lap shear
55
56 strength of the joints on aluminium substrates. While the neat adhesive fractured adhesively at
57
58 7.5 MPa, the adhesive containing 20 wt% EG GFG5 fractured fully cohesively at 11.1 MPa.
59
60 The change of the failure mode after addition of EG indicates a stronger adhesion between

1
2
3 aluminium and the adhesive that provides higher strength of the joint. Stronger adhesion may
4 be a result of better wetting of the substrate surface after addition of EG to the adhesive [30,
5
6
7 46]. This is a very interesting result compared to some previous works where the addition of
8
9
10 EG or GNP to adhesives led to lower tensile lap-shear strength on aluminium substrates [29-
11
12
13 30]. By using EG modified adhesives, higher adhesive fracture energy (mode I) on
14
15 aluminium substrates could be achieved compared to the neat adhesive. Nonetheless, the
16
17 values remained at the same level for all EG GFG5 modified adhesives. A distinct change of
18
19 the failure mode from adhesive (neat epoxy) through mixed (adhesive/cohesive) at 6 and 10
20
21 wt% EG GFG5 to fully cohesive failure mode at 20 wt% EG GFG5 in the adhesive could be
22
23
24 observed. Burst pressure tests on PP/graphite KS500 samples showed that EG GFG5-filled
25
26 adhesives can withstand a higher internal air pressure than the neat adhesive. This lead to an
27
28 important conclusion that EG modified adhesives can provide higher strength of the joint not
29
30 only on aluminium but on PP-substrates as well. Optical microscopy confirmed the uniform
31
32
33 distribution of EG particles within the adhesive.

34
35 In summary the paper showed that the addition of conductive EG into epoxy based adhesives
36
37 is a very promising approach to increase the thermal conductivity trough the joint as well as
38
39 the adhesion to aluminium and PP/EG substrates.
40
41
42
43

44 **Acknowledgment**

45 The authors thank the German Federal Ministry of Education and Research for financial support of
46
47 this work (project no. 01LY1512 and 01LY1307). We also thank our industry partners Mr. M. Jasch
48
49 (Protech GmbH, Pfullingen, Germany) for designing and Mr. Dr. T. Hickmann (Eisenhuth GmbH &
50
51 Co. KG, Osterode am Harz, Germany) for providing the mold for the burst pressure samples as well as
52
53 Mr. A. Cohnen (Institute of Plastics Processing, RWTH Aachen, Germany) for melt compounding of
54
55 the PP/graphite Timcal Timrex KS500 composites. The authors would like to thank Mr. H. Scheibner
56
57 and Mrs. K. Eichhorn for mechanical tests, Mrs. K. Arnhold for TGA measurements, Mrs. Ch.
58
59 Steinbach for particle size distribution measurements, Mr. B. Kretschmar for melt compounding of
60

1
2
3 the PP/EG GFG600 composites and Andreas Scholze (all from IPF Dresden) for injection moulding of
4
5 the burst pressure specimens.
6
7

8 **5. Literature**

- 9
10
11 1. Fu, Y.-X.; He, Z.-X.; Mo, D.-C.; Lu, S.-S., *Appl. Therm. Eng.* **2014**, *66* (1), 493-498.
12
13 2. Li, Y.; Wong, C. P., *Mater. Sci. Eng. R Rep.* **2006**, *51* (1), 1-35.
14
15 3. Reylek, R. S.; Thompson, K. C. Electrically and thermally conductive adhesive
16 transfer tape. US4606962, 19. August, 1986.
17
18 4. Ameen, J. G.; Korleski, J. E.; W. P. Mortimer, J.; Yokimcus, V. P. Thermally
19 conductive adhesive interface. US5591034, 7. January, 1997.
20
21 5. Schwarzbauer, H. Heat-conducting adhesive joint with an adhesive filled, porous heat
22 conductor. US6823915 B2, 30. November, 2004.
23
24 6. Larminie, J.; Dicks, A., *Fuel Cell Systems Explained*. 2nd ed.; John Wiley & Sons:
25 Chichester, England, 2003.
26
27 7. Rzeczowski, P.; Krause, B.; Pötschke, P., *Polymers* **2019**, *11* (3), 462.
28
29 8. Fuller, T. J.; Kumar, V. Fuel Cell Adhesive and process of making the same.
30 US20110281195 A1, 17. November, 2011.
31
32 9. Sekine, S. Adhesive material for fuel cell. US20130040221A1, 13 February 2013.
33
34 10. Miller, D. P.; Beutel, M. J.; Bhargava, S.; Reich, C. E. Integrated fuel cell assembly
35 and method of making. US20110318667 A1, 2011.
36
37 11. Farrington, S. Assembling bipolar plates for fuel cells using microencapsulated
38 adhesive. US9105883B2, 2015.
39
40 12. Sigler, D. R.; Schroth, J. G. Conductive adhesive bonding. US7510621 B2, 31. March,
41 2009.
42
43 13. Scherer, G. G., *Fuel Cells 1*. Springer-Verlag: Berlin Heidelberg, 2008.
44
45
46
47
48
49
50
51
52
53
54
55
56
57
58
59
60

14. Bolger, J. C. In *Prediction and measurement of thermal conductivity of diamond filled adhesives*, 1992 Proceedings 42nd Electronic Components & Technology Conference, 18-20 May; IEEE: 1992; pp 219-224.
15. Mirmira, S. R.; Marotta, E. E.; Fletcher, L. S., *J. Thermophys. Heat Transfer* **1997**, *11* (2), 141-145.
16. Teertstra, P. In *Thermal Conductivity and Contact Resistance Measurements for Adhesives*, ASME 2007 InterPACK Conference collocated with the ASME/JSME 2007 Thermal Engineering Heat Transfer Summer Conference, Vancouver, Canada, July 8-12; Vancouver, Canada, 2007; pp 381-388.
17. Wong, C. P.; Bollampally, R. S., *J. Appl. Polym. Sci.* **1999**, *74* (14), 3396-3403.
18. Fu, Y.-X.; He, Z.-X.; Mo, D.-C.; Lu, S.-S., *Int. J. Therm. Sci.* **2014**, *86*, 276-283.
19. Kim, J.; Yim, B.-s.; Kim, J.-m.; Kim, J., *Microelectron. Reliab.* **2012**, *52* (3), 595-602.
20. Kwon, Y.; Yim, B.-s.; Kim, J.; Kim, J., *Microelectron. Reliab.* **2011**, *51*, 812-818.
21. Debelak, B.; Lafdi, K., *Carbon* **2007**, *45* (9), 1727-1734.
22. Antunes, R. A.; de Oliveira, M. C. L.; Ett, G.; Ett, V., *J. Power Sources* **2011**, *196* (6), 2945-2961.
23. Planes, E.; Flandin, L.; Alberola, N., *Energy Procedia* **2012**, *20*, 311-323.
24. Kenig, S., *Processing of Polymer Nanocomposites*. Carl Hanser Verlag GmbH: München, 2019; p 517.
25. Burger, N.; Laachachi, A.; Ferriol, M.; Lutz, M.; Toniazzo, V.; Ruch, D., *Prog. Polym. Sci.* **2016**, *61*, 1-28.
26. Cahill, D. G.; Ford, W. K.; Goodson, K. E.; Mahan, G. D.; Majumdar, A.; Maris, H. J.; Merlin, R.; Phillpot, S. R., *J. Appl. Phys.* **2003**, *93* (2), 793-818.
27. Bader, M.; Maenz, T.; Schmiederer, D.; Kuehnert, I.; Leuteritz, A.; Heinrich, G., *Polymer Engineering & Science* **2015**, *55* (10), 2231-2236.
28. Swartz, E. T.; Pohl, R. O., *Rev. Mod. Phys.* **1989**, *61* (3), 605-668.

- 1
2
3 29. Kumar, R.; Mohanty, S.; Nayak, S. K., *SN Applied Sciences* **2019**, *1* (2), 180.
4
5 30. Moriche, R.; Prolongo, S. G.; Sánchez, M.; Jiménez-Suárez, A.; Chamizo, F. J.;
6 Ureña, A., *Int. J. Adhes. Adhes.* **2016**, *68*, 407-410.
7
8 31. Sihm, S.; Ganguli, S.; Roy, A. K.; Qu, L.; Dai, L., *Compos. Sci. Technol.* **2008**, *68* (3),
9 658-665.
10
11 32. Mukhopadhyay, P.; Gupta, R. K., *Graphite, graphene and their polymer composites*.
12 Taylor & Francis Group, LLC: Boca Raton, FL, US, 2013.
13
14 33. Habenicht, G., *Kleben: Grundlagen, Technologien, Anwendungen*. Springer-Verlag:
15 Berlin Heidelberg, 2006.
16
17 34. Ehrenstein, G. W., *Handbuch Kunststoff-Verbindungstechnik*. Carl Hanser Verlag:
18 München, 2004.
19
20 35. Gantayat, S.; Prusty, G.; Rout, D. R.; Swain, S. K., *New Carbon Mater.* **2015**, *30* (5),
21 432-437.
22
23 36. Lin, W.; Xi, X.; Yu, C., *Synthetic Metals* **2009**, *159* (7), 619-624.
24
25 37. Jojibabu, P.; Jagannatham, M.; Haridoss, P.; Janaki Ram, G. D.; Deshpande, A. P.;
26 Bakshi, S. R., *Composites, Part A* **2016**, *82*, 53-64.
27
28 38. Park, S. W.; Kim, B. C.; Lee, D. G., *J. Adhes. Sci. Technol.* **2009**, *23* (1), 95-113.
29
30 39. Gude, M. R.; Prolongo, S. G.; Gómez-del Río, T.; Ureña, A., *Int. J. Adhes. Adhes.*
31 **2011**, *31* (7), 695-703.
32
33 40. Khoramishad, H.; Khakzad, M., *J. Adhes.* **2018**, *94* (1), 15-29.
34
35 41. Mohamed, M.; Taheri, F., *J. Adhes. Sci. Technol.* **2017**, *31* (19-20), 2105-2123.
36
37 42. Bai, J. B.; Allaoui, A., *Composites, Part A* **2003**, *34* (8), 689-694.
38
39 43. Montazeri, A.; Javadpour, J.; Khavandi, A.; Tcharkhtchi, A.; Mohajeri, A., *Mater.*
40 *Des.* **2010**, *31* (9), 4202-4208.
41
42 44. Ghosh, P. K.; Kumar, K.; Chaudhary, N., *Composites, Part B* **2015**, *77*, 139-144.
43
44 45. Srivastava, V. K., *Mater. Des.* **2012**, *39*, 432-436.
45
46
47
48
49
50
51
52
53
54
55
56
57
58
59
60

- 1
2
3 46. Prolongo, S. G.; Gude, M. R.; Sanchez, J.; Ureña, A., *J. Adhes.* **2009**, *85* (4-5), 180-
4
5 199.
6
7 47. Krause, B.; Pötschke, P.; Hickmann, T., *AIP Conference Proceedings* **2019**, *2139*,
8
9 110006.
10
11 48. Krause, B.; Cohnen, A.; Pötschke, P.; Hickmann, T.; Koppler, D.; Proksch, B.;
12
13 Kersting, T.; Hopmann, C., *AIP Conference Proceedings* **2017**, *1914* (1), 030009.
14
15 49. Kraft, W. W., Betriebsfestigkeit: Auch Bauteile ermüden. *Kunststoffe* 2009, pp 108-
16
17 111.
18
19 50. Ganguli, S.; Roy, A. K.; Anderson, D. P., *Carbon* **2008**, *46* (5), 806-817.
20
21 51. Zhou, W.; Yu, D., *J. Appl. Polym. Sci.* **2010**, *118* (6), 3156-3166.
22
23 52. Abenojar, J.; Martínez, M. A.; Pantoja, M.; Velasco, F.; Del Real, J. C., *J. Adhes.*
24
25 **2012**, *88* (4-6), 418-434.
26
27 53. Lapique, F.; Redford, K., *Int. J. Adhes. Adhes.* **2002**, *22* (4), 337-346.
28
29 54. Zhong, W. H.; Li, J.; Lukehart, C. M.; Xu, L. R., *Polym. Compos.* **2005**, *26* (2), 128-
30
31 135.
32
33 55. Garton, A.; Stevenson, W. T. K.; Wang, S. P., *J. Polym. Sci., Part A: Polym. Chem.*
34
35 **1988**, *26* (5), 1377-1391.
36
37 56. Zheng, W.; Lu, X.; Wong, S.-C., *J. Appl. Polym. Sci.* **2004**, *91* (5), 2781-2788.
38
39 57. Yasmin, A.; Daniel, I. M., *Polymer* **2004**, *45* (24), 8211-8219.
40
41 58. Cordisco, F. A.; Zavattieri, P. D.; Hector, L. G.; Carlson, B. E., *Int. J. Solids Struct.*
42
43 **2016**, *83*, 45-64.
44
45
46
47
48
49
50
51
52
53
54
55
56
57
58
59
60

Table 1. Actual filler content in EG GFG5 modified epoxy adhesives obtained from TGA measurements.

Adhesive	Actual filler content in adhesive [wt%]
Epoxy + 6 wt% EG GFG5	6.1
Epoxy + 10 wt% EG GFG5	10.3
Epoxy + 20 wt% EG GFG5	20.3

Table 2. Thermal conductivity (TC) through the joint at different adhesive layer thickness.

Adhesive	TC adhesive [W/m·K]	Substrate	TC substrate [W/m·K]	Adhesive layer thickness [mm]	TC through the joint [W/m·K]
Epoxy resin Epikote MGS RIM 145	0.23 ± 0.01	PP + 60 wt% EG GFG 600	9.47 ± 0.33	0.1	2.09 ± 0.30
				0.3	1.54 ± 0.22
				0.5	0.87 ± 0.07

Table 3. Adhesive fracture energy of EG GFG5 modified adhesives on aluminium substrates.

Adhesive	Specimen No.	Fracture energy G_{IC} [J/m ²]	Fracture energy G_{IC} – mean value [J/m ²]	Failure mode
Epoxy	1	60.0	68.0 ± 23.1	adhesive
	2	50.0		
	3	94.0		
Epoxy/6 wt% EG	1	233.4	230.9 ± 37.4	mixed(predominantly adhesive)
	2	266.9		
	3	192.3		
Epoxy/10 wt% EG	2	266.4	246.3 ± 28.5	mixed (predominantly cohesive)
	3	226.1		
Epoxy/ 20 wt% EG	1	212.6	200.2 ± 20.4	cohesive
	2	176.6		
	3	211.4		

Table 4. Results of burst pressure test using different EG GFG5 modified adhesives and PP/graphite substrates.

Adhesive	Substrate	Tightness at air pressure 2 bar	Burst pressure test
Neat epoxy	Neat PP	OK	Failure at 5 bar
		OK	Failure at 3,5 bar
Neat epoxy	PP + 20 wt% graphite KS 500	OK	No failure at 8 bar
		OK	Failure at 4 bar
Neat epoxy	PP + 40 wt% graphite KS 500	OK	No failure at 8 bar
		OK	No failure at 8 bar
Neat epoxy	PP + 60 wt% graphite KS 500	OK	No failure at 8 bar
		OK	No failure at 8 bar
Epoxy + 6 wt% EG GFG5	Neat PP	OK	Failure at 6 bar
		OK	Failure at 5,5 bar
Epoxy + 10 wt% EG GFG5	Neat PP	OK	Failure at 8 bar after approx. 30 sec
		OK	Failure at 8 bar after approx. 30 sec
Epoxy + 20 wt% EG GFG5	Neat PP	OK	Failure at 7 bar
		OK	Failure at 7 bar

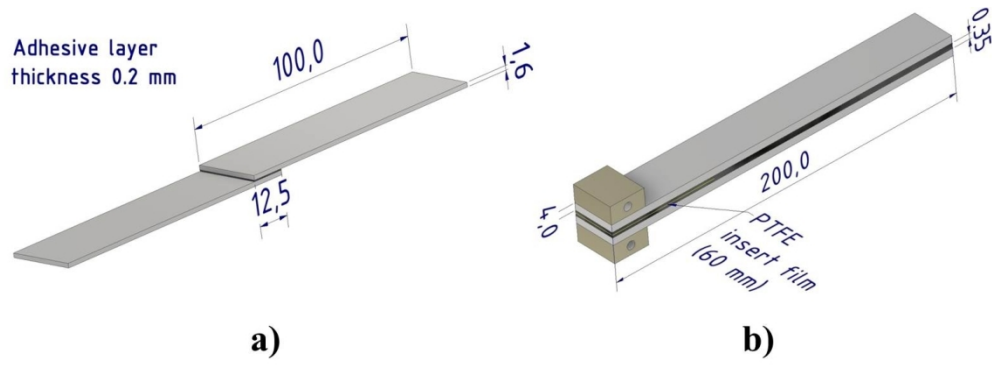


Figure 1. Samples for (a) lap-shear test and (b) adhesive fracture energy determination made of aluminium substrates.

133x49mm (300 x 300 DPI)

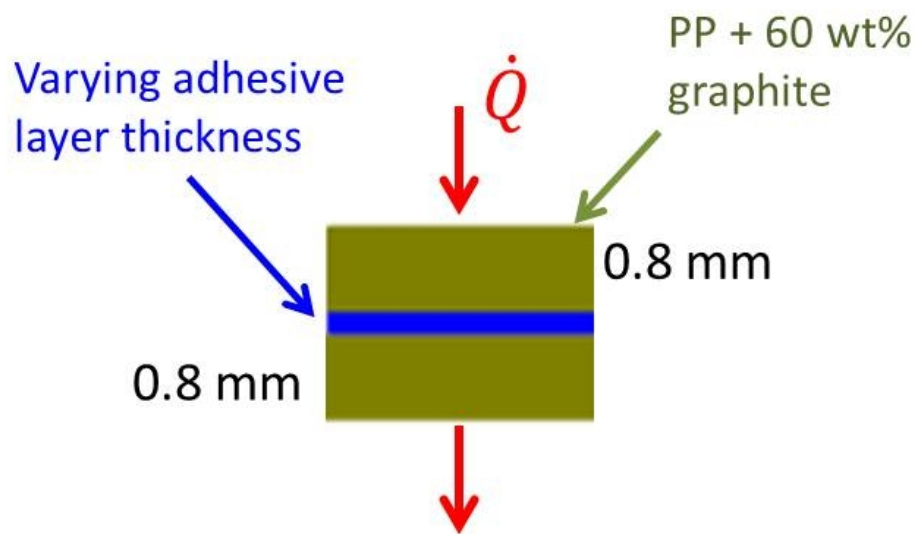


Figure 2. Graphic representation of the specimen used for the measurements of the thermal conductivity through the joint.

57x34mm (300 x 300 DPI)

1
2
3
4
5
6
7
8
9
10
11
12
13
14
15
16
17
18
19
20
21
22
23
24
25
26
27
28
29
30
31
32
33
34
35
36
37
38
39
40
41
42
43
44
45
46
47
48
49
50
51
52
53
54
55
56
57
58
59
60

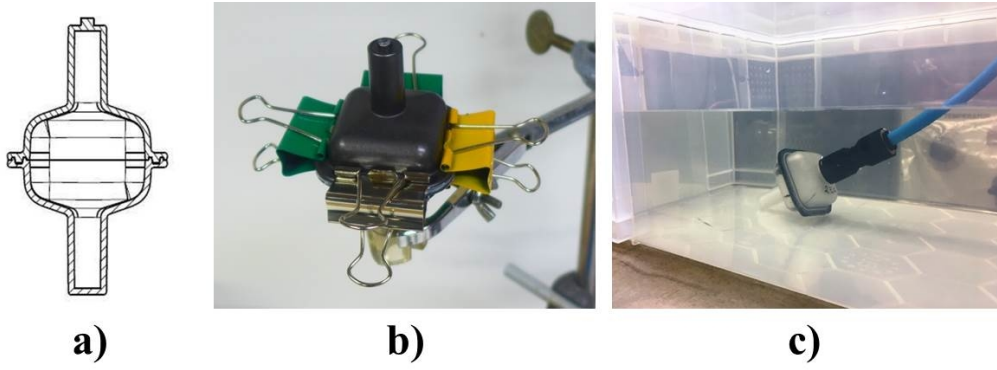


Figure 3. Burst pressure samples (a) 2D drawing, (b) adhesive joining, (c) gas-tightness test in water.

97x38mm (300 x 300 DPI)

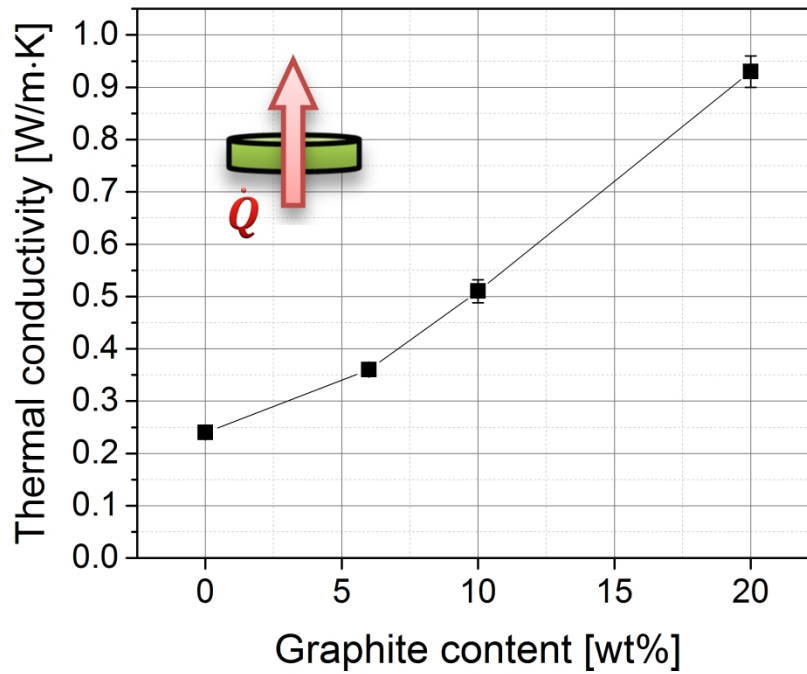


Figure 4. Thermal conductivity of adhesives filled with different contents of EG GFG5.

272x208mm (300 x 300 DPI)

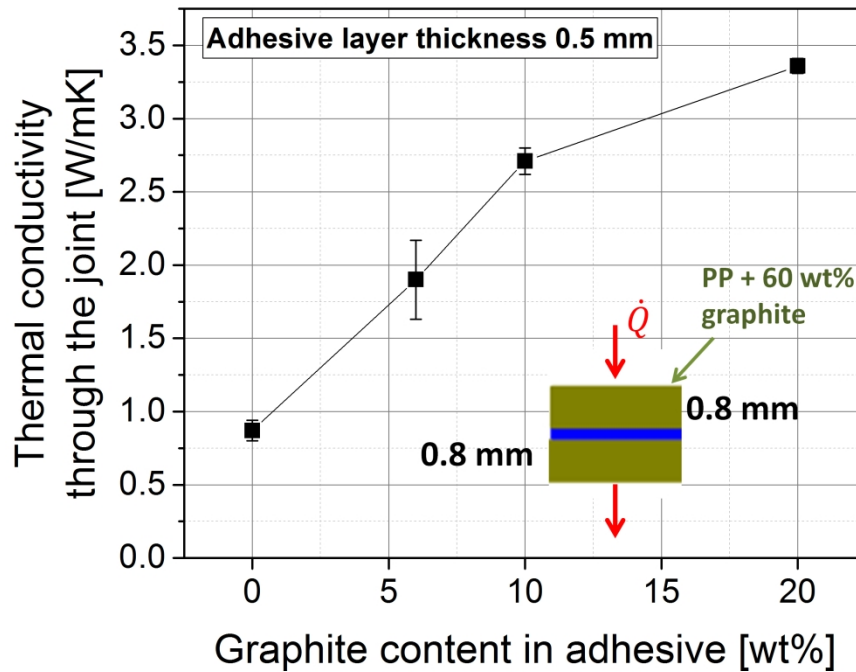


Figure 5. Thermal conductivities through the joint with adhesives filled with different contents of EG GFG5.

272x208mm (300 x 300 DPI)

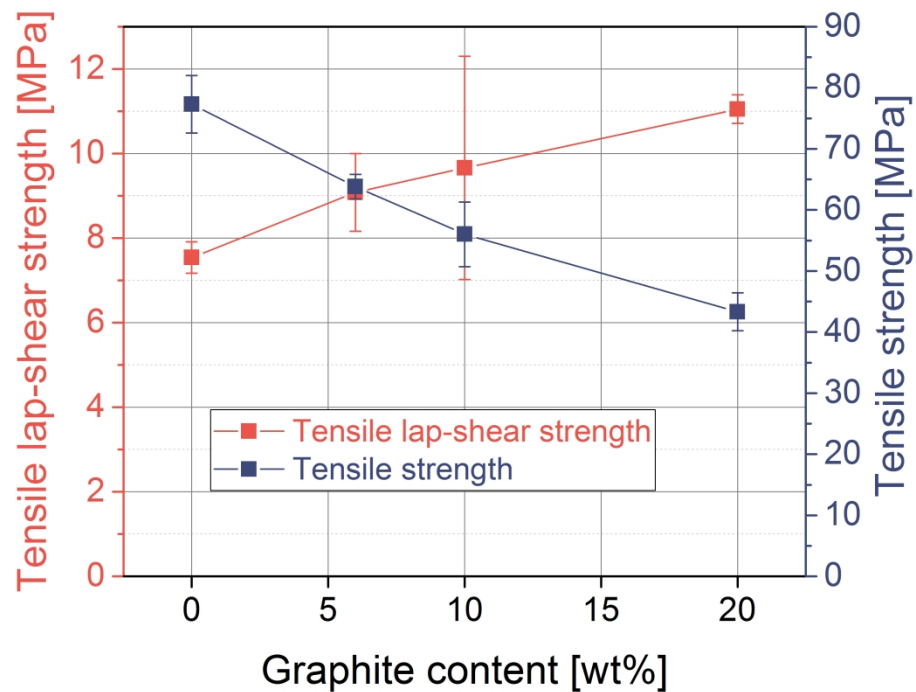


Figure 6. Tensile strength of EG GFG5 modified adhesives and tensile lap-shear strength of adhesively joined aluminium substrates with EG GFG5 modified adhesives.

272x208mm (300 x 300 DPI)

1
2
3
4
5
6
7
8
9
10
11
12
13
14
15
16
17
18
19
20
21
22
23
24
25
26
27
28
29
30
31
32
33
34
35
36
37
38
39
40
41
42
43
44
45
46
47
48
49
50
51
52
53
54
55
56
57
58
59
60

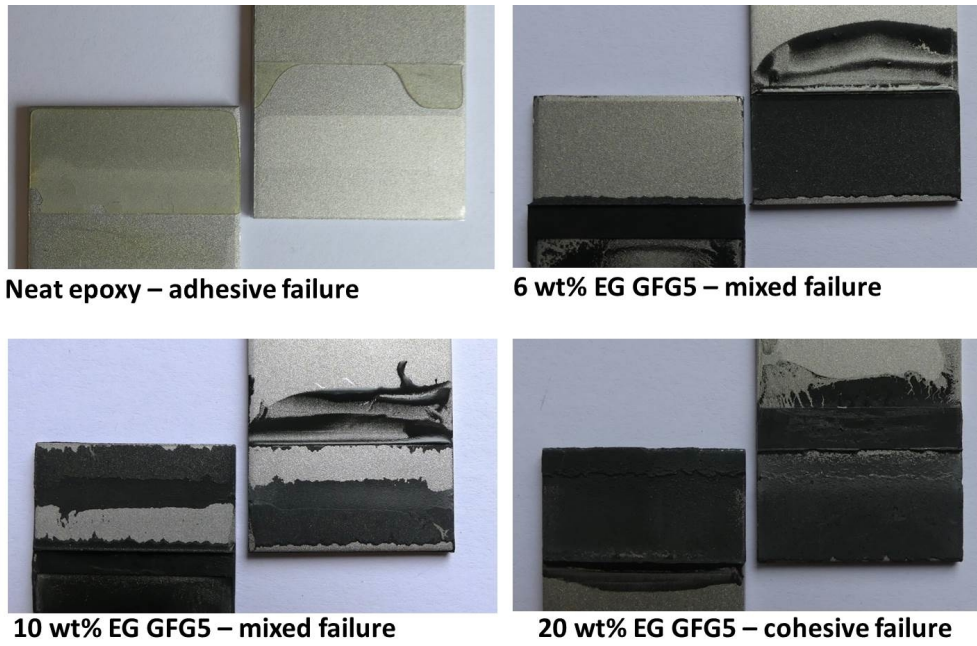


Figure 7. Fracture surfaces of adhesives filled with EG GFG5 after lap-shear tests.

121x80mm (300 x 300 DPI)

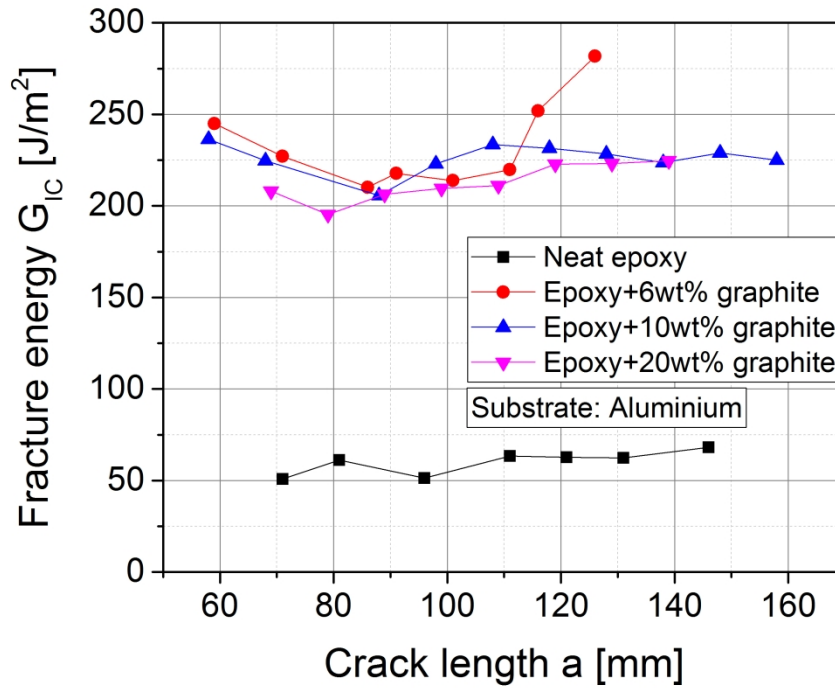


Figure 8. Fracture energies G_{IC} of single samples of the adhesives on aluminium substrates in dependence on crack length a .

272x208mm (300 x 300 DPI)

1
2
3
4
5
6
7
8
9
10
11
12
13
14
15
16
17
18
19
20
21
22
23
24
25
26
27
28
29
30
31
32
33
34
35
36
37
38
39
40
41
42
43
44
45
46
47
48
49
50
51
52
53
54
55
56
57
58
59
60

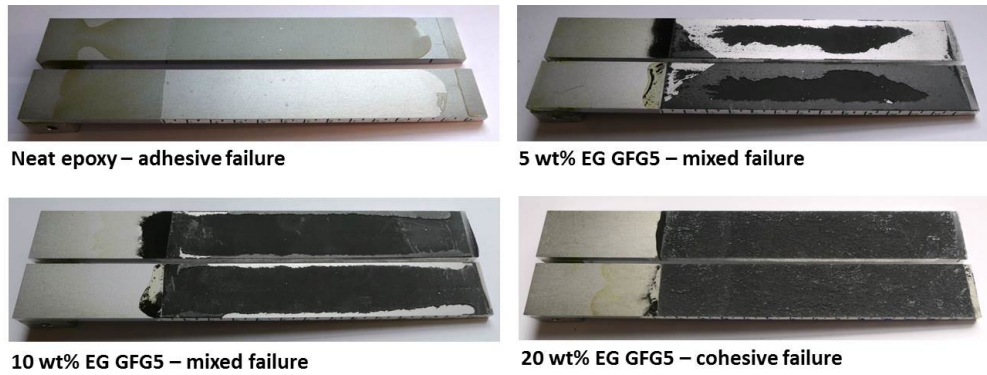


Figure 9. Fracture surface of neat epoxy adhesive and EG GFG5 modified epoxy adhesives from fracture toughness mode 1 test.

109x42mm (300 x 300 DPI)

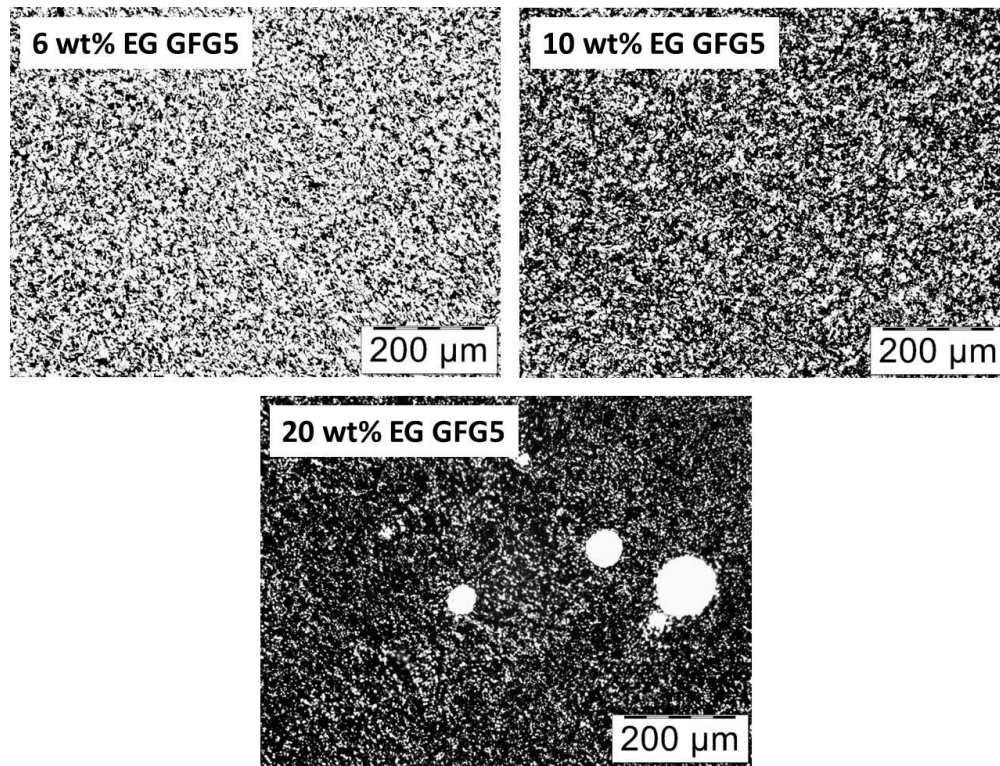


Figure 10. Transmission light micrographs of thin cross section of modified adhesives containing 6 wt% (top left), 10 wt% (top right) and 20 wt% EG GFG5 (bottom).

108x82mm (300 x 300 DPI)